Nano Modification of Hard Coatings with Ions

Branko Skoric, Aleksandar Miletic, Pal Terek,
Lazar Kovacevic & Milan Kukuruzovic
University of Novi Sad
Faculty of technical Sciences
Center for Surface Engineering and Nanotechnology
Novi Sad, Serbia
skoricb@uns.ac.rs

***Abstract*— In this paper, we present the results of a study of TiN films which are deposited by a Physical Vapor Deposition and Ion Beam Assisted Deposition. In the present investigation the subsequent ion implantation was provided with N^{5+} ions. The ion implantation was applied to enhance the mechanical properties of surface. The film deposition process exerts a number of effects such as crystallographic orientation, morphology, topography, densification of the films. A variety of analytic techniques were used for characterization, such as scratch test, calo test, SEM, AFM, XRD and EDAX.**

***Index Terms*: Hard coatings, ion implantation, synthesis, microstructure, nanohardness.**

I. INTRODUCTION

The film deposition process exerts a number of effects such as crystallographic orientation, morphology, topography, densification of the films. The optimization procedure for coated parts could be more effective, knowing more about the fundamental physical and mechanical properties of a coating. In this research are present the results of a study of the relationship between the process, composition, microstructure and nanohardness of duplex TiN coatings and modified with ion implantation.

A duplex surface treatment involves the sequential application of two surface technologies to produce a surface composition with combined properties [1]. A typical duplex process involves plasma nitriding and the coating treatment of materials. In the paper are presented characteristics of hard coatings deposited by PVD (physical vapor deposition) and IBAD (ion beam assisted deposition). The duplex coating method can improve further of the tribological properties and load-bearing capacity of materials beyond metals. The synthesis of the TiN film by IBAD has been performed by irradiation of Ar ions. The evolution of the microstructure from porous and columnar grains to dense packed grains is accompanied by changes in mechanical and physical properties. Subsequent ion implantation was provided with N^{5+} ions. Ion implantation has the capabilities of producing new compositions and structures unattainable by conventional means. Implantation may result in changes in the surface properties of a material, including hardness, wear, coefficient of friction and other properties.

Thin hard coatings deposited by physical vapor deposition (PVD), e.g. titanium nitride (TiN) are frequently used to improve tribological performance in many engineering applications [2]. In many cases single coating cannot solve the wear problems [3]. The combination of nitriding and hard coating allows the production of duplex coatings, which are distinguished by a high resistance against complex loads, since the advantages of both individual processes are combined here. The film deposition process exerts a number of effects such as crystallographic orientation, morphology, topography, densification of the films. The optimization procedure for coated parts could be more effective, knowing more about the fundamental physical and mechanical properties of a coating, their interdependence and their influence on the wear behavior. The effects on the structure as well as mechanical and tribological properties of the films were investigated in detail in the present research.

The results were correlated with properties determined from mechanical and tribological characterization. Therefore, by properly selecting the processing parameters, well-adherent TiN films with low friction coefficient, low wear rate and high hardness can be obtained on engineering steel substrates, and show a potential for tribological applications.

The duplex surface treatment was used to enhance adhesion strength and hardness of hard coatings. The depth of nanopenetration provides an indirect measure of the area of contact at full load and thus hardness is obtained by dividing the maximum applied load with the contact area. Micro hardness testing, Vickers micro hardness, is dependent on visual resolution of the residual indent for accurate measurement. The diagonal of the indent, which is the key for hardness determination, is sometimes very hard to resolve if the load is low enough to avoid cracking and again this would be much more difficult if cracking occurs at high load within the indent site.

In the nanoindentation technique, hardness and Young's modulus can be determined by the Oliver and Pharr method [4], where hardness (H) can be defined as: $H = \frac{P_{\max}}{A}$, where P_{max} is maximum applied load, and A is contact area at maximum load. In nanoindentation, the Young's Modulus, E, can be obtained from:

$$\frac{1}{E_r} = \frac{1-\nu^2}{E} + \frac{1-\nu_i^2}{E_i} \quad (1)$$

IJRS

Where v_i=Poisson ratio of the diamond indenter (0.07) and Ei=Young's modulus of the diamond indenter.
On the other hand, in the Vickers micro hardness tester, the hardness can be calculated by measuring the residual indent area with the help of an optical microscope and the value is fully dependent on the visual resolution of the indentation.

Therefore, in recent years, a number of measurements have been made in which nanoindentation and AFM have been combined.

II. EXPERIMENTAL

The substrate material used was high speed steel type S 6-5-2. Prior to deposition the substrate was mechanically polished to a surface roughness of 0.12 μm (R_a). The specimens were first austenized, quenched and than tempered to the final hardness of 850 HV. In order to produce good adhesion of the coating, the substrates were plasma nitrided at low pressure (1×10^{-3} Pa), prior to deposition of the coating. The PVD treatment was performed in a Balzers Sputron installation with rotating specimen. The gas flow into the deposition chamber was controlled by mass flow meters and the partial pressures of argon and nitrogen were measured. The deposition parameters were as follows: Base pressure in the chamber was 1×10^{-5} mbar, bias voltage U_b=1 kV, discharge current I_d=50 mA, substrate temperature T_s=200 °C, target to substrate distance d_s–t=120 mm. The partial pressure of Ar during deposition was P_{Ar}=(3.1–6.6)×10^{-6} mbar and partial pressure of N_2 was P_{N2}=6.0×10^{-6}–1.1×10^{-5} mbar. Deposition rate a_D=0.1 nm/s. Prior to entering the deposition chamber the substrates were cleaned.

The other samples were produced with IBAD technology in DANFYSIK chamber. The IBAD system consists of an e-beam evaporation source for evaporating Ti metal and 5-cm-diameter Kaufman ion source for providing argon ion beam. Base pressure in the IBAD chamber was 1×10^{-6} mbar. The partial pressure of Ar during deposition was $(3.1–6.6) \times 10^{-6}$ mbar and partial pressure of N_2 was 6.0×10^{-6}–1.1×10^{-5} mbar. The ion energy (E_{Ar}=1.5–2 keV), ion beam incident angle (15°), target to substrate distance d_s–t=360 mm, and substrate temperature T_s=200 °C, were chosen as the processing variables. Deposition rate a_D=0.05–0.25 nm/s. Quartz crystal monitor was used to gauge the approximate thickness of the film. Additional analyze the thickness of coatings, the ball crater method (calo-test), allows prompt and sufficiently precise results to be obtained. After deposition, the samples were irradiated with 22 keV N^{2+} ions at room temperature (RT). N^{2+} ions were supplied by an electron cyclotron resonance (ECR) ion source. The implanted fluences were in the range from 0.6×10^{17} to 1×10^{17} ions/cm^2

A pure titanium intermediate layer with a thickness of about 50nm has been deposited first for all the coatings to enhance the interfacial adhesion to the substrates. After deposition, the samples were irradiated with 120 keV, N^{5+} ions at room temperature (RT). The Ion Source is a multiply charged heavy ion injector, based on the electron cyclotron resonance effect (ECR). The implanted fluencies were in the range from 0.6×10^{17} to 1×10^{17} ions/cm^2.

The mechanical properties on coated samples were characterized using a Nanohardness Tester (NHT) developed by CSM Instruments, Switzerland. Nanoindentation testing was carried out with applied loads in the range of 10 to 20 mN. The nanohardness tester was calibrated by using fused silica samples for a range of operating conditions. A Berkovich diamond indenter was used for all the measurements. The tip radius of the indenter was approximately 50 nm and the displacement resolution of the machine was 0.03 nm. The data was processed using proprietary software to produce load–displacement curves and the mechanical properties were calculated using the Oliver and Pharr method. At least ten measurements were made at each load on the coated sample. Measurement of hardness was also carried out using a conventional Vickers microhardness tester.

The Nano-Hardness tester uses an already established method where a Berkovich indenter tip with a known geometry is driven into a specific site of the material to be tested, by applying an increasing normal load. For each loading/unloading cycle, the applied load value is plotted with respect to the corresponding position of the indenter. The resulting load/displacement curves provide data specific to the mechanical nature of the material under examination. Established models are used to calculate quantitative hardness and modulus values for such data. The NHT is especially suited to load and penetration depth measurements at nanometer length scales. The maximum indentation depth for measuring H and E was fixed at one tenth of the coating thickness.

The analysis of the indents was performed by Atomic Force Microscope (AFM). Acoustic Emission (AE) is an important tool for the detection and characterization of failures in the framework of non-destructive testing. The analyzed AE signal was obtained by a scratching test designed for adherence evaluation. Scratch tests were performed under controlled conditions with a device that consisted of a loaded probe with a diamond indenter moving linearly along the sample with a constant speed and continuously increasing force. The steadily increasing contact load causes tensile stress behind the indenter tip and compressive stress ahead of the cutting tip. Detection of elastic waves generated as a result of the formation and propagation of microcracks. The AE sensor is insensitive to mechanical vibration frequencies of the instrument. This enables the force fluctuations along the scratch length to be followed, and the friction coefficient to be measured. The scratch tester equipment with an acoustic sensor (CSM-REVETEST) was used.

X-ray diffraction studies were undertaken in an attempt to determine the phases present, and perhaps an estimate of grain size from line broadening. The determination of phases was realized by X-ray diffraction using PHILIPS APD 1700 X-ray diffractometer. The X-ray sources were from CuKα with wavelength of 15.443 nm (40 kV, 40 mA) at speed

IJRS

0.9°/min. The surface roughness was measured using stylus type (Talysurf Taylor Hobson) instruments. The most popular experimental XRD approach to the evaluation of residual stresses in polycrystalline materials is the $\sin^2 \psi$ method. For each selected (hkl) crystallographic direction, diffraction data are collected at different ψ tilting angles. The method requires a θ-2θ scan for every ψ angle around the selected diffraction peak and, in order to emphasize the peak shifts, it is important to work at the highest possible 2θ angle.

III. RESULTS

The nitrogen to metal ratio, EDX, table 1, is stoichiometries for IBAD technology and something smaller from PVD. For sample with additional ion implantation, value is significantly different, smaller. It is possibly diffused from the layer of TiN to the interface. The TiN coatings only show a golden surface and after ion implantation the color is dark golden

Table I: ATOMIC RATIO N/TI IN COATING

	Coating	Ratio N/Ti (atomic)
1	IBAD	1.00
2	PVD	0.98
3	PVD/III	0.89

The analysis of the indents was performed by Atomic Force Microscope (Figure 1a).It can be seen, from cross section of an indent during indentation, that the indents are regularly shaped with the slightly concave edges tipically seen where is significant degree of elastic recovery.(Figure 1b).

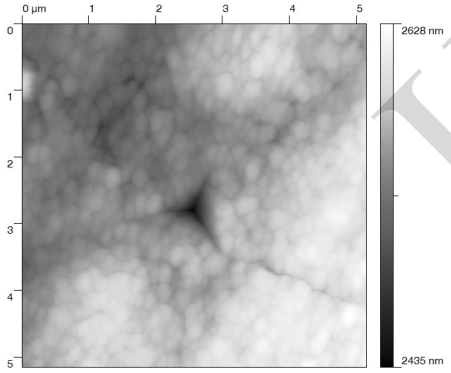


Fig. 1.a: AFM image of a nanoindentation

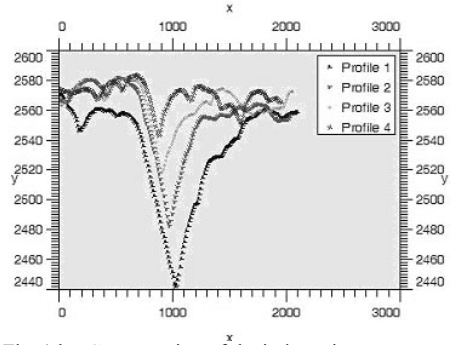


Fig. 1.b: Cross-section of the indentation

All the results of nanohardness are obtained with the Oliver & Pharr method and using a supposed sample Poisson's ratio of 0.3 for modulus calculation.

The nanohardness values and microhardness are shown in table 2.

Table II: SURFACE MICROHARDNESS (HV0.03) AND NANOHARDNESS (LOAD-10MN).

Unit	pn/IBAD	PVD	pn/PVD/II	Fused Silica
Vickers	2007	3028	3927	943
GPa	21.6	32.6	42.6	10,1

For each measurement, the penetration (Pd), the residual penetration (Rd), the acoustic emission (AE) and the frictional force are recorded versus the normal load. The breakdown of the coatings was determined both by AE signal analysis and optical and scanning electron microscopy.
AE permits an earlier detection, because the shear stress is a maximum at certain depth beneath the surface, where a subsurface crack starts. Critical loads are presents in Table 3..

Table III: CRITICAL LOAD FOR DIFFERENT TYPE OF COATING.

	pn/TiN(IBAD)	pn/TiN(PVD)
Lc1	-	23
Lc2	100	54
Lc3	138	108

The critical load Lc1 corresponds to the load inducing the first crack on the coating. No cracks were observed on sample 1.The critical load Lc2 corresponds to the load inducing the partial delamination of the coating. The critical load Lc3 corresponds to the load inducing the full delamination of the coating. AE permits an earlier detection, because the shear stress is a maximum at certain depth beneath the surface, where a subsurface crack starts (PVD), figure 2.

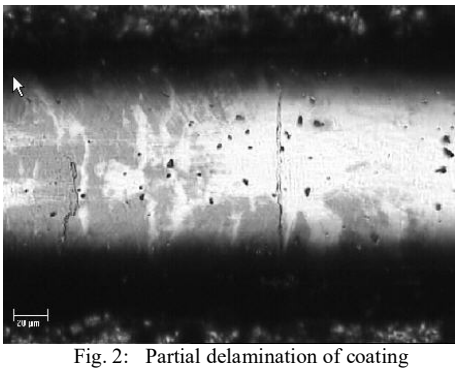


Fig. 2: Partial delamination of coating

It was found that the plasma-nitriding process enhanced the coating to substrates adhesion. In some places of hard coatings cohesive failure of the coating and the delamination of the coating was observed (Fig. 3).

IJRS

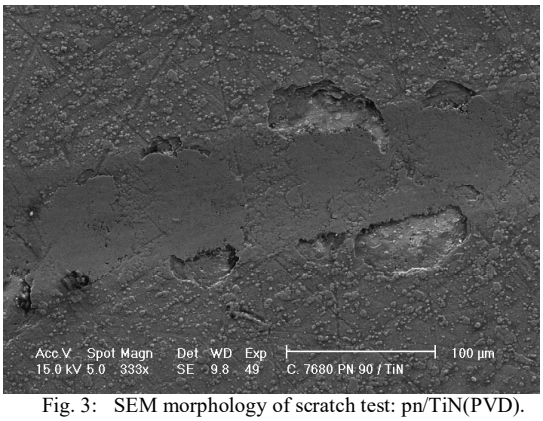


Fig. 3: SEM morphology of scratch test: pn/TiN(PVD).

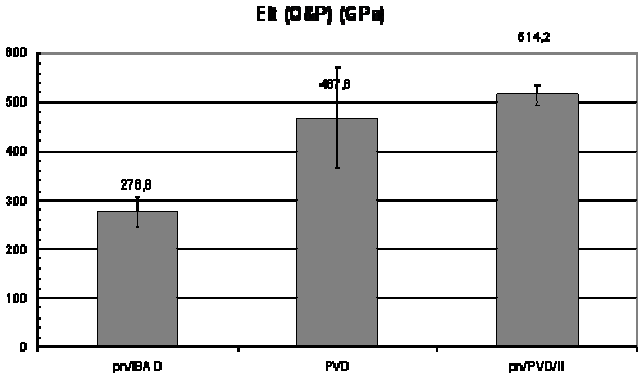


Fig. 4: Young's elastic module.

The nanoindentation elastic modulus was calculated using the Oliver–Pharr data analysis procedure. The individual values of E are the different for all measurements, figure 4.

The errors related to the measurements and estimations were different and for duplex coating with ion implantation is less than 4%. Good agreement could be achieved between the E_c values and nanohardness.

The tribological behaviour of the coatings was studied also by means of pin-on-ring contact configuration in dry sliding conditions, described elsewhere [5]. The friction coefficient of sample with duplex coating with additional ion implantation, is presented in Fig. 5

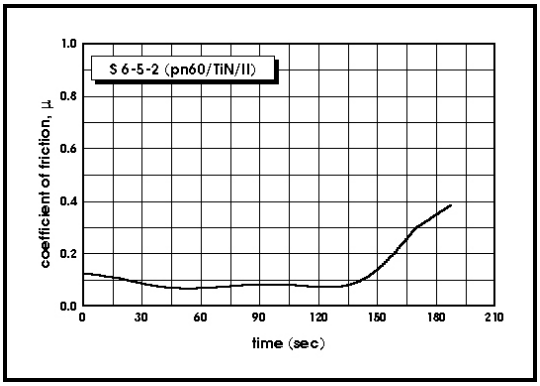


Fig. 5: Friction Coefficient of pn/TiN/II

The width of column is derived from the width of the diffraction peaks (Figure 6), (λ=0.154nm, θ=62.5° and β=0.056rad), and it is 70 nm.

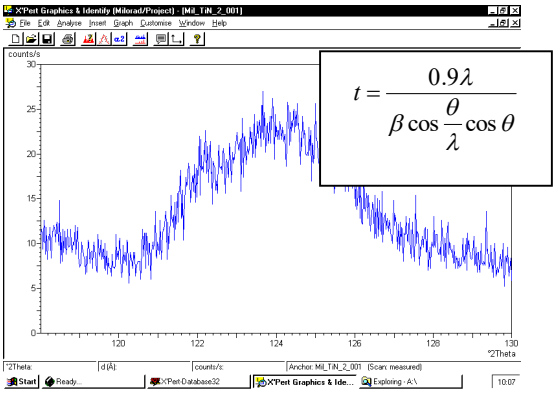


Fig. 6: XRD diffraction peak of TiN(422).

The stress determination follows the conventional $\sin^2\psi$ method. Stress determination was performed using a PHILIPS XPert diffractometer. The (422) diffraction peak was recorded in a 2θ interval between 118° and 130°, with tilting angle: ψ_o^1=0°, ψ_o^2=18.75°, ψ_o^3=27.03°, ψ_o^4=33.83°, ψ_o^5=40°. A typical result for compact film, with residual stresses σ = -4.28Gpa, has TiN(PVD).

IV. DISCUSSION

A hardness increase is observed for implanted samples. This can be attributed to iron nitride formation in the near surface regions. The standard deviation of the results is relatively important due to the surface roughness of the samples. Because the thickness of the TiN coatings presented here is sufficiently large, which for all coatings is about 2900 nm (TiN-PVD), the hardness measurements will not be affected by the substrate, as in three times thinner (900 nm TiN-IBAD).

The individual values of E are the different for all measurements. The errors related to the measurements and estimations were different and for duplex coating with ion implantation is less than 4%. Good agreement could be achieved between the E_c values and nanohardness.

The wear resistance of the TiN coating was obviously improved by the presence of a nitride interlayer. Such an improvements is probably due to the adequate bonding between the nitrided layer and substrate. Energy depressive analyze with X-ray (EDAX), of the transfer layer showed that the transfer layer consists of small amount of counter material (adhesive wear), Fig.7.

IJRS

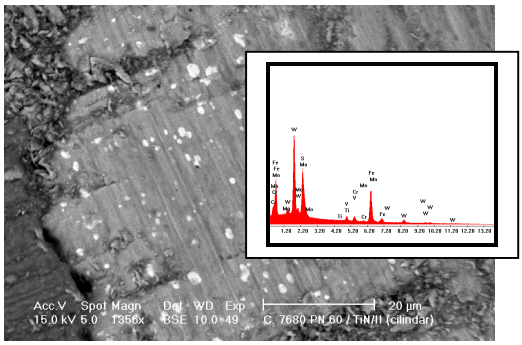


Fig. 7: SEM micrograph of wear track (BSE), with wear debris and EDAX image of wear debris.

It is generally expected that an increase in hardness results in an increase in wear resistance.

The topography of TiN coatings was investigated SEM (Figure 8).

The PVD coating process did not significantly change roughness. For the practical applications of IBAD coatings, it is important to know that the roughness of the surface decreased slightly after deposition (from Ra=0.19 μm to Ra=0.12 μm).

The curves of friction coefficient are clearly reproducible and distinctively show a lower rise in friction coefficient for the composite (pn/TiN) coated specimens and much more for sample with additional ion implantation (under 0.1). It is generally expected that an increase in hardness results in an increase in wear resistance.

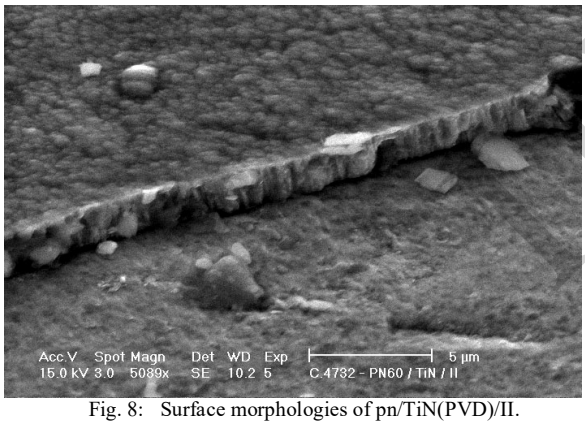


Fig. 8: Surface morphologies of pn/TiN(PVD)/II.

The formation of TiN by IBAD has its origin in a kinetically controlled growth. The nitrogen atoms occupy the octahedric sites in varying number according to the energy that these atoms possess to cross the potential barriers created by the surrounding titanium anions. The ion bombardment is believed to enhance the mobility of the atoms on the sample surface. XRD analysis revealed the presence of only one phase, δ-TiN, and there is no evidence for other phases, such as Ti_2N, could be found. The ε-Ti_2N does not lead to an improvement in the tribological behavior.

The coating morphology was evaluated using the well-known structure zone model of Thornton. All observed morphologies, figure 8, are believed to be from region of zone I (PVD) and from the border of region zone T (IBAD).

It has been suggested [6]. That the transition from open porous coatings with low microhardness and rough surface, often in tensile stress to dense coatings films with greater microhardness, smooth surface occurs at a well defined critical energy delivered to the growing film.

V. CONCLUSIONS

It was concluded that the formation of a plasma nitrided layer at low pressure, beneath a hard coating, is important in determining the use of hard coating. The experimental results indicated that the mechanical hardness is elevated by penetration of nitrogen, whereas the Young's modulus is significantly elevated. Nitrogen ion implantation leads to the formation of a highly wear resistant and hard surface layer.

Coatings developed under this project should demonstrate performance that exceeds that of PVD coatings. Nitrogen implantation into hard TiN coatings increases the surface hardness and significantly reduces the tendency of the coatings to form microcracks when subjected to loads or stresses.

The present coating method can produce dance structures, high hardness and the high critical load values can be achieved. Tribological tests confirm that these composite coatings are wear resistant and provide very low friction coefficient

The above findings show that deposition process and the resulting coating properties depend strongly on the additional ion bombardment.

ACKNOWLEDGMENT

The authors gratefully acknowledge the financial support Science and Technological Development of Autonomous Province of Vojvodina

REFERENCES

[1] J.C.A. Batista, C. Godoy and A. Matthews, A. Leyland, "Developments Towards Producing Well Adherent Duplex PAPVD Coatings", *Surface Engineering*, 9, 37-43., 2003.

[2] Y. Sun and T. Bell, "Plasma surface engineering of low alloy stee" l, *Mater. Sci. Eng*., A 140, 419-434., 1991.

[3] H. Haufmann,, "Industrial applications of plasma and ion surface engineering" *Surface and Coatings Technology*, 74-75, 23-28..1988.

[4] Pharr, G.M., Oliver, W.C., Brotzen, F.R., "On the generality of the relationship among contact stiffness, contact area, and elastic modulus during indentation", *J. Mater. Res*., 7, 613, 1992.

[5] B. Škorić and D. Kakaš, "Influence of plasma nitriding on mechanical and tribological properties of steel with subsequent PVD surface treatments", *Thin Solid Films*, 317, 486-489., 1998.

[6] L. Combadiere, J. Machet, "Reactive magnetron sputtering deposition of TiN films", *Surface and Coating Technology*, 88, 17-27., 1996.